

¹ **Critical transitions and the fragmenting of global forests**

² **Leonardo A. Saravia^{1 3}, Santiago R. Doyle¹, Benjamin Bond-Lamberty²**

³ 1. Instituto de Ciencias, Universidad Nacional de General Sarmiento, J.M. Gutierrez 1159 (1613), Los
⁴ Polvorines, Buenos Aires, Argentina.

⁵ 2. Pacific Northwest National Laboratory, Joint Global Change Research Institute at the University of
⁶ Maryland–College Park, 5825 University Research Court #3500, College Park, MD 20740, USA

⁷ 3. Corresponding author e-mail: lsaravia@ungs.edu.ar

⁸ **keywords:** Forest fragmentation, early warning signals, percolation, power-laws, MODIS, critical transitions

⁹ **Running title:** Critical fragmentation in global forest

¹⁰ **Abstract**

¹¹ 1. Forests provide critical habitat for many species, essential ecosystem services, and are coupled to
¹² atmospheric dynamics through exchanges of energy, water and gases. One of the most important
¹³ changes produced in the biosphere is the replacement of forest areas with human dominated landscapes.
¹⁴ This usually leads to fragmentation, altering the sizes of patches, the structure and function of the
¹⁵ forest. Here we studied the distribution and dynamics of forest patch sizes at a global level, examining
¹⁶ signals of a critical transition from an unfragmented to a fragmented state.

¹⁷ 2. We used MODIS vegetation continuous field to estimate the forest patches at a global level and de-
¹⁸ fined wide regions of connected forest across continents and big islands. We search for critical phase
¹⁹ transitions, where the system state of the forest changes suddenly at a critical point in time; this
²⁰ implies an abrupt change in connectivity that causes an increased fragmentation level. We studied the
²¹ distribution of forest patch sizes and the dynamics of the largest patch over the last fourteen years,
²² as the conditions that indicate that a region is near a critical fragmentation threshold are related to
²³ patch size distribution and temporal fluctuations of the largest patch.

²⁴ 3. We found some evidence that allows us to analyze fragmentation as a critical transition: most regions
²⁵ followed a power-law distribution over the 14 years. We also found that the Philippines region probably
²⁶ went through a critical transition from a fragmented to an unfragmented state. Only the tropical forest
²⁷ of Africa and South America met the criteria to be near a critical fragmentation threshold.

28 4. This implies that human pressures and climate forcings might trigger undesired effects of fragmentation,
29 such as species loss and degradation of ecosystems services, in these regions. The simple criteria
30 proposed here could be used as an early warning to estimate the distance to a fragmentation threshold
31 in forest around the globe and a predictor of a planetary tipping point.

32 Introduction

33 Forests are one of the most important biomes on earth, providing habitat for a large proportion of species
34 and contributing extensively to global biodiversity (Crowther et al., 2015). In the previous century human
35 activities have influenced global bio-geochemical cycles (Bonan, 2008; Canfield, Glazer, & Falkowski, 2010),
36 with one of the most dramatic changes being the replacement of 40% of Earth's formerly biodiverse land
37 areas with landscapes that contain only a few species of crop plants, domestic animals and humans (J. A.
38 Foley et al., 2011). These local changes have accumulated over time and now constitute a global forcing
39 (Barnosky et al., 2012).

40 Another global scale forcing that is tied to habitat destruction is fragmentation, which is defined as the
41 division of a continuous habitat into separated portions that are smaller and more isolated. Fragmentation
42 produces multiple interwoven effects: reductions of biodiversity between 13% and 75%, decreasing forest
43 biomass, and changes in nutrient cycling (Haddad et al., 2015). The effects of fragmentation are not only
44 important from an ecological point of view but also that of human activities, as ecosystem services are deeply
45 influenced by the level of landscape fragmentation (Mitchell et al., 2015).

46 Ecosystems have complex interactions between species and present feedbacks at different levels of organiza-
47 tion (Gilman, Urban, Tewksbury, Gilchrist, & Holt, 2010), and external forcings can produce abrupt changes
48 from one state to another, called critical transitions (Scheffer et al., 2009). These abrupt state shifts cannot
49 be linearly forecasted from past changes, and are thus difficult to predict and manage (Scheffer et al., 2009).
50 Such 'critical' transitions have been detected mostly at local scales (S. R. Carpenter et al., 2011; Drake &
51 Griffen, 2010), but the accumulation of changes in local communities that overlap geographically can prop-
52 agate and theoretically cause an abrupt change of the entire system at larger scales (Barnosky et al., 2012).
53 Coupled with the existence of global scale forcings, this implies the possibility that a critical transition could
54 occur at a global scale (C. Folke et al., 2011; Rockstrom et al., 2009).

55 Complex systems can experience two general classes of critical transitions (R V Solé, 2011). In so-called first
56 order transitions, a catastrophic regime shift that is mostly irreversible occurs because of the existence of
57 alternative stable states (Scheffer et al., 2001). This class of transitions is suspected to be present in a variety
58 of ecosystems such as lakes, woodlands, coral reefs (Scheffer et al., 2001), semi-arid grasslands (Brandon T.
59 Bestelmeyer et al., 2011), and fish populations (Vasilakopoulos & Marshall, 2015). They can be the result of
60 positive feedback mechanisms (Villa Martín, Bonachela, Levin, & Muñoz, 2015); for example, fires in some
61 forest ecosystems were more likely to occur in previously burned areas than in unburned places (Kitzberger,
62 Aráoz, Gowda, Mermoz, & Morales, 2012).

63 The other class of critical transitions are continuous or second order transitions (Ricard V. Solé & Bascompte,
64 2006). In these cases, there is a narrow region where the system suddenly changes from one domain to another,
65 with the change being continuous and in theory reversible. This kind of transitions were suggested to be
66 present in tropical forest (S. Pueyo et al., 2010), semi-arid mountain ecosystems (McKenzie & Kennedy,
67 2012), tundra shrublands (Naito & Cairns, 2015). The transition happens at a critical point where we can
68 observe a distinctive spatial pattern: scale invariant fractal structures characterized by power law patch
69 distributions (Stauffer & Aharony, 1994).

70 There are several processes that can convert a catastrophic transition to a second order transitions (Villa
71 Martín et al., 2015). These include stochasticity, such as demographic fluctuations, spatial heterogeneities,
72 and/or dispersal limitation. All these components are present in forest around the globe (Filotas et al.,
73 2014; Fung, O'Dwyer, Rahman, Fletcher, & Chisholm, 2016; Seidler & Plotkin, 2006), and thus continuous
74 transitions might be more probable than catastrophic transitions. Moreover there is some evidence of recovery
75 in some systems that supposedly suffered an irreversible transition produced by overgrazing (Brandon T
76 Bestelmeyer, Duniway, James, Burkett, & Havstad, 2013; J. Y. Zhang, Wang, Zhao, Xie, & Zhang, 2005)
77 and desertification (Allington & Valone, 2010).

78 The spatial phenomena observed in continuous critical transitions deal with connectivity, a fundamental
79 property of general systems and ecosystems from forests (Ochoa-Quintero, Gardner, Rosa, de Barros Ferraz,
80 & Sutherland, 2015) to marine ecosystems (Leibold & Norberg, 2004) and the whole biosphere (Lenton &
81 Williams, 2013). When a system goes from a fragmented to a connected state we say that it percolates (R
82 V Solé, 2011). Percolation implies that there is a path of connections that involves the whole system. Thus
83 we can characterize two domains or phases: one dominated by short-range interactions where information
84 cannot spread, and another in which long range interactions are possible and information can spread over
85 the whole area. (The term “information” is used in a broad sense and can represent species dispersal or
86 movement.)

87 Thus, there is a critical “percolation threshold” between the two phases, and the system could be driven close
88 to or beyond this point by an external force; climate change and deforestation are the main forces that could
89 be the drivers of such a phase change in contemporary forests (Bonan, 2008; Haddad et al., 2015). There
90 are several applications of this concept in ecology: species' dispersal strategies are influenced by percolation
91 thresholds in three-dimensional forest structure (Ricard V Solé, Bartumeus, & Gamarra, 2005), and it has
92 been shown that species distributions also have percolation thresholds (He & Hubbell, 2003). This implies
93 that pushing the system below the percolation threshold could produce a biodiversity collapse (J. Bascompte
94 & Solé, 1996; Pardini, Bueno, Gardner, Prado, & Metzger, 2010; Ricard V. Solé, Alonso, & Saldaña, 2004);

95 conversely, being in a connected state (above the threshold) could accelerate the invasion of forest into prairie
96 (Loehle, Li, & Sundell, 1996; Naito & Cairns, 2015).

97 One of the main challenges with systems that can experience critical transitions—of any kind—is that the
98 value of the critical threshold is not known in advance. In addition, because near the critical point a small
99 change can precipitate a state shift of the system, they are difficult to predict. Several methods have been
100 developed to detect if a system is close to the critical point, e.g. a deceleration in recovery from perturbations,
101 or an increase in variance in the spatial or temporal pattern (Boettiger & Hastings, 2012; S. R. Carpenter
102 et al., 2011; Dai, Vorselen, Korolev, & Gore, 2012; Hastings & Wysham, 2010).

103 The existence of a critical transition between two states has been established for forest at global scale in
104 different works (Hirota, Holmgren, Nes, & Scheffer (2011); Verbesselt et al. (2016); Wuyts, Champneys, &
105 House (2017)). It was not probed, but is generally believed, that this constitutes a first order catastrophic
106 transition. The regions where forest can grow are not distributed homogeneously, there are demographic
107 fluctuations in forest growth and disturbances produced by human activities. Due to new theoretical advances
108 (Villa Martín, Bonachela, & Muñoz, 2014; Villa Martín et al., 2015) all these factors imply that if these were
109 first order transitions they will be converted or observed as second order continuous transitions. From this
110 basis we applied indices derived from second order transitions to global forest cover dynamics.

111 In this study, our objective is to look for evidence that forests around the globe are near continuous critical
112 point that represent a fragmentation threshold. We use the framework of percolation to first evaluate if
113 forest patch distribution at a continental scale is described by a power law distribution and then examine
114 the fluctuations of the largest patch. The advantage of using data at a continental scale is that for very
115 large systems the transitions are very sharp (R V Solé, 2011) and thus much easier to detect than at smaller
116 scales, where noise can mask the signals of the transition.

117 Methods

118 Study areas definition

119 We analyzed mainland forests at a continental scale, covering the whole globe, by delimiting land areas with
120 a near-contiguous forest cover, separated with each other by large non-forested areas. Using this criterion,
121 we delimited the following forest regions. In America, three regions were defined: South America temperate
122 forest (SAT), subtropical and tropical forest up to Mexico (SAST), and USA and Canada forest (NA). Europe
123 and North Asia were treated as one region (EUAS). The rest of the delimited regions were South-east Asia

124 (SEAS), Africa (AF), and Australia (OC). We also included in the analysis islands larger than 10^5 km^2 . The
125 mainland region has the number 1 e.g. OC1, and the nearby islands have consecutive numeration (Appendix
126 S4, figure S1-S6).

127 Forest patch distribution

128 We studied forest patch distribution in each defined area from 2000 to 2015 using the MODerate-resolution
129 Imaging Spectroradiometer (MODIS) Vegetation Continuous Fields (VCF) Tree Cover dataset version 051
130 (C. DiMiceli et al., 2015). This dataset is produced at a global level with a 231-m resolution, from 2000
131 onwards on an annual basis. There are several definition of forest based on percent tree cover (J. O. Sexton
132 et al., 2015); we choose a range from 20% to 30% threshold in 5% increments to convert the percentage
133 tree cover to a binary image of forest and non-forest pixels. This range is centered in the definition used by
134 the United Nations' International Geosphere-Biosphere Programme (Belward, 1996), and studies of global
135 fragmentation (Haddad et al., 2015) and includes the range used in other studies of critical transitions (C.
136 Xu et al., 2016). Using this range we try to avoid the errors produced by low discrimination of MODIS VCF
137 between forest and dense herbaceous vegetation at low forest cover and the saturation of MODIS VCF in
138 dense forests (J. O. Sexton et al., 2013). We repeat all the analysis described below for this set of thresholds,
139 except in some specific cases. Patches of contiguous forest were determined in the binary image by grouping
140 connected forest pixels using a neighborhood of 8 forest units (Moore neighborhood).

141 Percolation theory

142 A more in-depth introduction to percolation theory can be found elsewhere (Stauffer & Aharony, 1994) and
143 a review from an ecological point of view is available (B. Oborny, Szabó, & Meszéna, 2007). Here, to explain
144 the basic elements of percolation theory we formulate a simple model: we represent our area of interest by a
145 square lattice and each site of the lattice can be occupied—e.g. by forest—with a probability p . The lattice
146 will be more occupied when p is greater, but the sites are randomly distributed. We are interested in the
147 connection between sites, so we define a neighborhood as the eight adjacent sites surrounding any particular
148 site. The sites that are neighbors of other occupied sites define a patch. When there is a patch that connects
149 the lattice from opposite sides, it is said that the system percolates. When p is increased from low values, a
150 percolating patch suddenly appears at some value of p called the critical point p_c .

151 Thus percolation is characterized by two well defined phases: the unconnected phase when $p < p_c$ (called
152 subcritical in physics), in which species cannot travel far inside the forest, as it is fragmented; in a general

153 sense, information cannot spread. The second is the connected phase when $p > p_c$ (supercritical), species
154 can move inside a forest patch from side to side of the area (lattice), i.e. information can spread over the
155 whole area. Near the critical point several scaling laws arise: the structure of the patch that spans the area
156 is fractal, the size distribution of the patches is power-law, and other quantities also follow power-law scaling
157 (Stauffer & Aharony, 1994).

158 The value of the critical point p_c depends on the geometry of the lattice and on the definition of the
159 neighborhood, but other power-law exponents only depend on the lattice dimension. Close to the critical
160 point, the distribution of patch sizes is:

161 (1) $n_s(p_c) \propto s^{-\alpha}$

162 where $n_s(p)$ is the number of patches of size s . The exponent α does not depend on the details of the
163 model and it is called universal (Stauffer & Aharony, 1994). These scaling laws can be applied for landscape
164 structures that are approximately random, or at least only correlated over short distances (Gastner, Oborny,
165 Zimmermann, & Pruessner, 2009). In physics this is called “isotropic percolation universality class”, and
166 corresponds to an exponent $\alpha = 2.05495$. If we observe that the patch size distribution has another exponent
167 it will not belong to this universality class and some other mechanism should be invoked to explain it.
168 Percolation thresholds can also be generated by models that have some kind of memory (Hinrichsen, 2000;
169 Ódor, 2004): for example, a patch that has been exploited for many years will recover differently than a
170 recently deforested forest patch. In this case, the system could belong to a different universality class, or in
171 some cases there is no universality, in which case the value of α will depend on the parameters and details
172 of the model (Corrado, Cherubini, & Pennetta, 2014).

173 To illustrate these concepts, we conducted simulations with a simple forest model with only two states: forest
174 and non-forest. This type of model is called a “contact process” and was introduced for epidemics (Harris,
175 1974), but has many applications in ecology (Gastner et al., 2009; Ricard V. Solé & Bascompte, 2006). A
176 site with forest can become extinct with probability e , and produce another forest site in a neighborhood
177 with probability c . We use a neighborhood defined by an isotropic power law probability distribution. We
178 defined a single control parameter as $\lambda = c/e$ and ran simulations for the subcritical fragmentation state
179 $\lambda < \lambda_c$, with $\lambda = 2$, near the critical point for $\lambda = 2.5$, and for the supercritical state with $\lambda = 5$ (see
180 supplementary data, gif animations).

181 **Patch size distributions**

182 We fitted the empirical distribution of forest patches calculated for each of the thresholds on the range
183 we previously mentioned. We used maximum likelihood (Clauset, Shalizi, & Newman, 2009; Goldstein,
184 Morris, & Yen, 2004) to fit four distributions: power-law, power-law with exponential cut-off, log-normal,
185 and exponential. We assumed that the patch size distribution is a continuous variable that was discretized
186 by remote sensing data acquisition procedure.

187 We set a minimal patch size (X_{min}) at nine pixels to fit the patch size distributions to avoid artifacts at patch
188 edges due to discretization (Weerman et al., 2012). Besides this hard X_{min} limit we set due to discretization,
189 the power-law distribution needs a lower bound for its scaling behavior. This lower bound is also estimated
190 from the data by maximizing the Kolmogorov-Smirnov (KS) statistic, computed by comparing the empirical
191 and fitted cumulative distribution functions (Clauset et al., 2009). For the log-normal model we constrain
192 the values of the μ parameter to positive values, this parameter controls the mode of the distribution and
193 when is negative most of the probability density of the distribution lies outside the range of the forest patch
194 size data (Limpert, Stahel, & Abbt, 2001).

195 To select the best model we calculated corrected Akaike Information Criteria (AIC_c) and Akaike weights for
196 each model (Burnham & Anderson, 2002). Akaike weights (w_i) are the weight of evidence in favor of model
197 i being the actual best model given that one of the N models must be the best model for that set of N
198 models. Additionally, we computed a likelihood ratio test (Clauset et al., 2009; Vuong, 1989) of the power
199 law model against the other distributions. We calculated bootstrapped 95% confidence intervals (Crawley,
200 2012) for the parameters of the best model; using the bias-corrected and accelerated (BCa) bootstrap (Efron
& Tibshirani, 1994) with 10000 replications.

202 **Largest patch dynamics**

203 The largest patch is the one that connects the highest number of sites in the area. This has been used
204 extensively to indicate fragmentation (R. H. Gardner & Urban, 2007; Ochoa-Quintero et al., 2015). The
205 relation of the size of the largest patch S_{max} to critical transitions has been extensively studied in relation
206 to percolation phenomena (Bazant, 2000; Botet & Ploszajczak, 2004; Stauffer & Aharony, 1994), but seldom
207 used in ecological studies (for an exception see Gastner et al. (2009)). When the system is in a connected
208 state ($p > p_c$) the landscape is almost insensitive to the loss of a small fraction of forest, but close to the
209 critical point a minor loss can have important effects (B. Oborny et al., 2007; Ricard V. Solé & Bascompte,
210 2006), because at this point the largest patch will have a filamentary structure, i.e. extended forest areas

211 will be connected by thin threads. Small losses can thus produce large fluctuations.

212 One way to evaluate the fragmentation of the forest is to calculate the proportion of the largest patch against
213 the total area (Keitt, Urban, & Milne, 1997). The total area of the regions we are considering (Appendix S4,
214 figures S1-S6) may not be the same than the total area that the forest could potentially occupy, thus a more
215 accurate way to evaluate the weight of S_{max} is to use the total forest area, that can be easily calculated
216 summing all the forest pixels. We calculate the proportion of the largest patch for each year, dividing S_{max}
217 by the total forest area of the same year: $RS_{max} = S_{max}/\sum_i S_i$. This has the effect of reducing the S_{max}
218 fluctuations produced due to environmental or climatic changes influences in total forest area. When the
219 proportion RS_{max} is large (more than 60%) the largest patch contains most of the forest so there are fewer
220 small forest patches and the system is probably in a connected phase. Conversely, when it is low (less than
221 20%), the system is probably in a fragmented phase (Saravia & Momo, 2017). As we calculated these largest
222 patch indices for different thresholds, the values of the total forest area and the value of S_{max} are lower as
223 threshold is higher, we expect that the value of RS_{max} will change and probably be lower at high thresholds.
224 To define if a region will be in a connected or unconnected state we used the RS_{max} of the highest threshold
225 (40%) which is more conservative to evaluate the risk of fragmentation and includes the most dense forest
226 area. Additionally if RS_{max} is a good indicator of the fragmented or unfragmented state of the forest and
227 these are the two alternative states for the critical transition the RS_{max} distribution of frequencies should be
228 bimodal (Brandon T. Bestelmeyer et al., 2011); so we apply the Hartigan's dip test that measures departures
229 from unimodality (J. A. Hartigan & Hartigan, 1985).

230 The RS_{max} is a useful qualitative index that does not tell us if the system is near or far from the critical
231 transition; this can be evaluated using the temporal fluctuations. We calculate the fluctuations around the
232 mean with the absolute values $\Delta S_{max} = S_{max}(t) - \langle S_{max} \rangle$, using the proportions of RS_{max} . To characterize
233 fluctuations we fitted three empirical distributions: power-law, log-normal, and exponential, using the same
234 methods described previously. We expect that large fluctuation near a critical point have heavy tails (log-
235 normal or power-law) and that fluctuations far from a critical point have exponential tails, corresponding to
236 Gaussian processes (Rooij, Nash, Rajaraman, & Holden, 2013). As the data set spans 16 years, it is probable
237 that will do not have enough power to reliably detect which distribution is better (Clauset et al., 2009). To
238 improve this we used the same likelihood ratio test we used previously (Clauset et al., 2009; Vuong, 1989);
239 if the p-value obtained to compare the best distribution against the others we concluded that there is not
240 enough data to decide which is the best model. We generated animated maps showing the fluctuations of
241 the two largest patches at 30% threshold, to aid in the interpretations of the results.

242 A robust way to detect if the system is near a critical transition is to analyze the increase in variance of

the density (Benedetti-Cecchi, Tamburello, Maggi, & Bulleri, 2015). It has been demonstrated that the variance increase in density appears when the system is very close to the transition (Corrado et al., 2014), thus practically it does not constitute an early warning indicator. An alternative is to analyze the variance of the fluctuations of the largest patch ΔS_{max} : the maximum is attained at the critical point but a significant increase occurs well before the system reaches the critical point (Corrado et al., 2014; Saravia & Momo, 2017). In addition, before the critical fragmentation, the skewness of the distribution of ΔS_{max} should be negative, implying that fluctuations below the average are more frequent. We characterized the increase in the variance using quantile regression: if variance is increasing the slopes of upper or/and lower quartiles should be positive or negative.

All statistical analyses were performed using the GNU R version 3.3.0 (R Core Team, 2015), to fit the distributions of patch sizes we used the Python package powerlaw (Alstott, Bullmore, & Plenz, 2014). For the quantile regressions we used the R package quantreg (Koenker, 2016). Image processing was done in MATLAB r2015b (The Mathworks Inc.). The complete source code for image processing and statistical analysis, and the patch size data files are available at figshare <http://dx.doi.org/10.6084/m9.figshare.4263905>.

Results

The figure 1 shows an example of the distribution of the biggest 200 patches for years 2000 and 2014, this distribution is highly variable, but the biggest patch usually maintains its place. Sometimes the biggest patch breaks and then big fluctuations in its size are observed, as we will analyze below. Smaller patches can merge or break more easily so they enter or leave the list of 200, and this is why there is a color change across years.

The power law distribution was selected as the best model in 99% of the cases (Figure S7). In a small number of cases (1%) the power law with exponential cutoff was selected, but the value of the parameter α was similar by ± 0.03 to the pure power law (Table S1, and model fit data table). Additionally the patch size where the exponential tail begins is very large, thus we used the power law parameters for this cases (region EUAS3,SAST2). In finite-size systems the favored model should be the power law with exponential cut-off, because the power-law tails are truncated to the size of the system (Stauffer & Aharony, 1994). This implies that differences between the two kinds of power law models should be small. We observed that phenomena: when the pure power-law model is selected as the best model the likelihood ratio test shows that in 64% of the cases the differences with power law with exponential cutoff are not significant ($p\text{-value}>0.05$); in these cases the differences between the fitted α for both models are less than 0.001. Instead the likelihood ratio

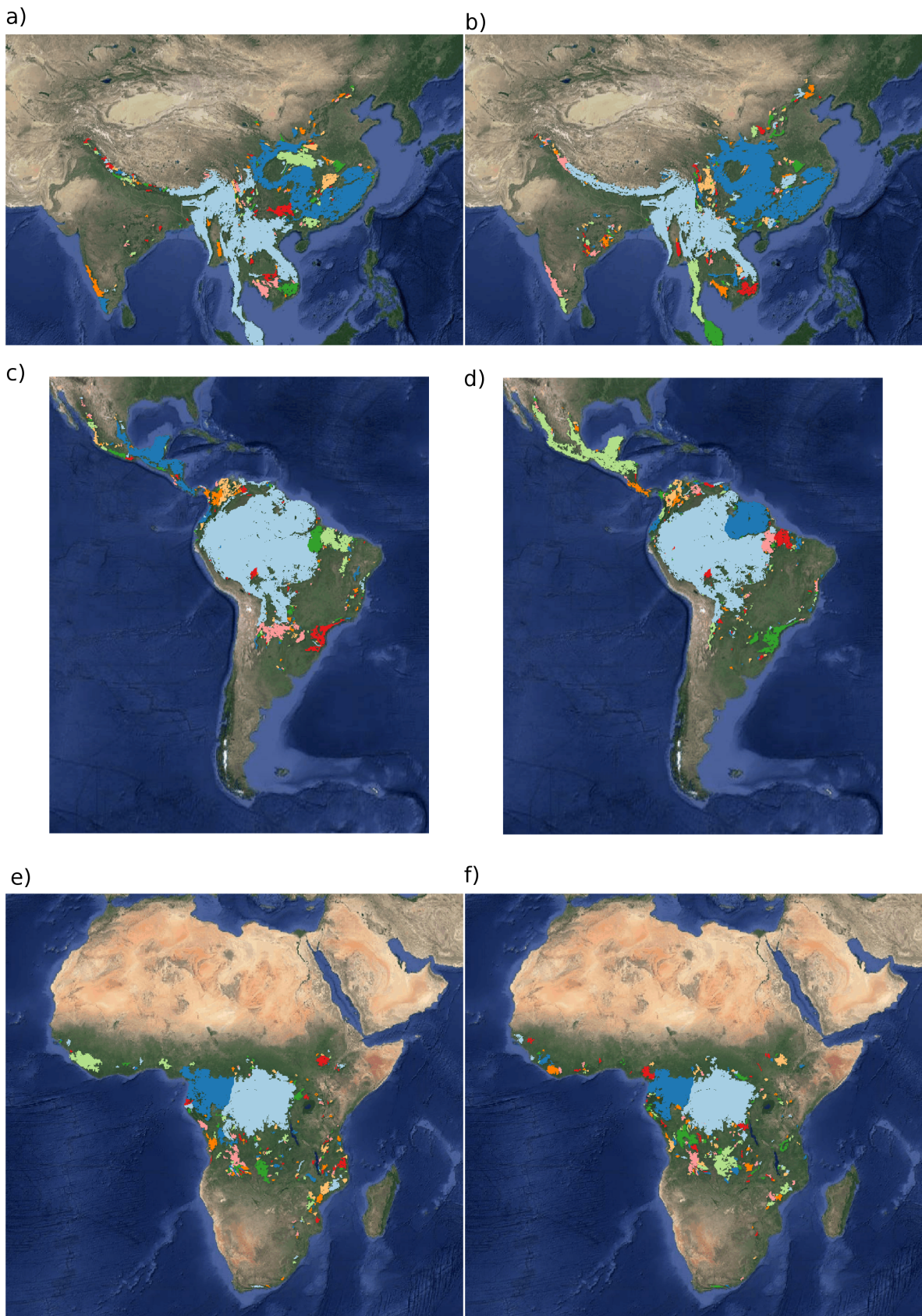


Figure 1: Forest patch distributions for continental regions for the years 2000 and 2014. The images are the 200 biggest patches, showed at a coarse pixel scale of 2.5 Km. The regions are: a) & b) southeast Asia; c) & d) South America subtropical and tropical and e) & f) Africa mainland, for the years 2000 and 2014 respectively. The color palette was chosen to discriminate different patches and do not represent patch size.

273 test clearly differentiates the power law model from the exponential model (100% cases p-value<0.05), and
274 the log-normal model (90% cases p-value<0.05).

275 The global mean of the power-law exponent α is 1.967 and the bootstrapped 95% confidence interval is 1.964
276 - 1.970. Besides that, the global values for each threshold are different, because their confidence intervals
277 do not overlap, and their range goes from 1.90 to 2.00 (Table S1). Analyzing the biggest regions (Figure
278 1, Table S2) the north hemisphere (EUAS1 & NA1) have similar values of α (1.97, 1.98), pantropical areas
279 have different α with greatest values for South America (SAST1, 2.01) and in descending order Africa (AF1,
280 1.946) and Southeast Asia (SEAS1, 1.895). With greater α the fluctuations of patch sizes are lower and vice
281 versa (M. E. J. Newman, 2005).

282 We calculated the total areas of forest and the largest patch S_{max} by year for different thresholds; as expected
283 these two values increase for smaller thresholds (Table S3). We expect less variations in the largest patch
284 relative to total forest area RS_{max} (Figure S9); in ten cases it keeps near or higher than 60% (EUAS2, NA5,
285 OC2, OC3, OC4, OC5, OC6, OC8, SAST1, SAT1) over the 25-35 range or more. In four cases it keeps
286 around 40% or less at least over the 25-30% range (AF1, EUAS3, OC1, SAST2) and in six cases there is
287 a crossover from more than 60% to around 40% or less (AF2, EUAS1, NA1, OC7, SEAS1, SEAS2). This
288 confirms the criteria of using the most conservative threshold value of 40% to interpret RS_{max} with regard
289 to the fragmentation state of the forest. The frequency of RS_{max} showed bimodality (Figure 3) and the dip
290 test rejected unimodality ($D = 0.0416$, p-value = 0.0003), which also indicates RS_{max} as a good index to
291 study the fragmentation state of the forest.

292 The RS_{max} for regions with more than 10^7 km² of forest is shown in figure 4. South America tropical and
293 subtropical (SAST1) is the only region with an average close to 60%, the other regions are below 30%. Eurasia
294 mainland (EUAS1) has the lowest value near 20%. For regions with less total forest area (Figure S10, Table
295 S3), Great Britain (EUAS3) has the lowest proportion less than 5%, Java (OC7) and Cuba (SAST2) are
296 under 25%, while other regions such as New Guinea (OC2), Malaysia/Kalimantan (OC3), Sumatra (OC4),
297 Sulawesi (OC5) and South New Zealand (OC6) have a very high proportion (75% or more). Philippines
298 (SEAS2) seems to be a very interesting case because it seems to be under 30% until the year 2007, fluctuates
299 around 30% in years 2008-2010, then jumps near 60% in 2011-2013 and then falls again to 30%, this seems
300 an example of a transition from a fragmented state to a unfragmented one (figure S10).

301 We analyzed the distributions of fluctuations of the largest patch relative to total forest area ΔRS_{max} and
302 the fluctuations of the largest patch ΔS_{max} . Besides the Akaike criteria identified different distributions as
303 the best, in most cases the Likelihood ratio test is not significant thus the data is not enough to determine

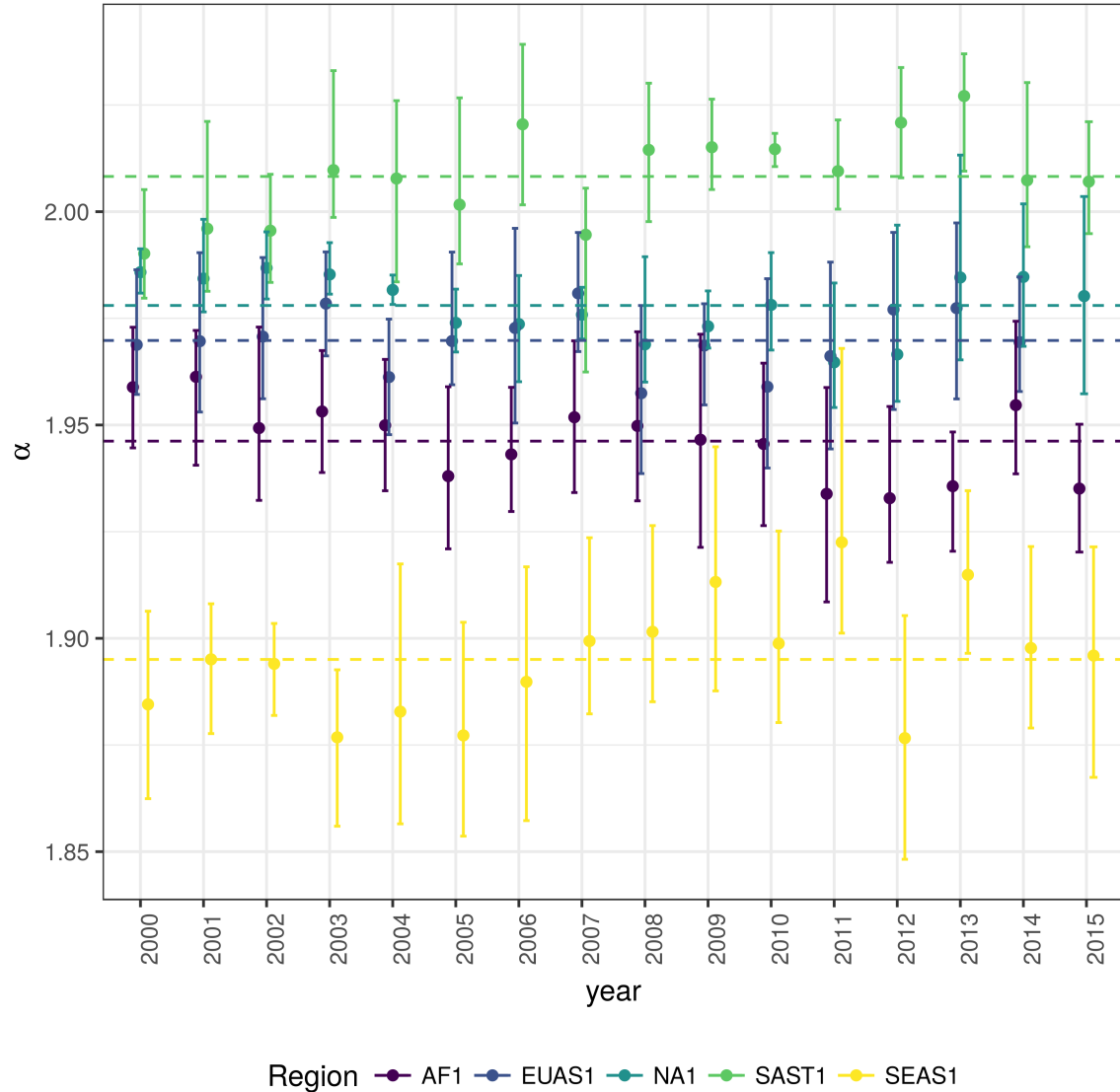


Figure 2: Power law exponents (α) of forest patch distributions for regions with total forest area $> 10^7 \text{ km}^2$. Dashed horizontal lines are the means by region, with 95% confidence interval error bars estimated by bootstrap resampling. The regions are AF1: Africa mainland, EUAS1: Eurasia mainland, NA1: North America mainland, SAST1: South America subtropical and tropical, SEAS1: Southeast Asia mainland.

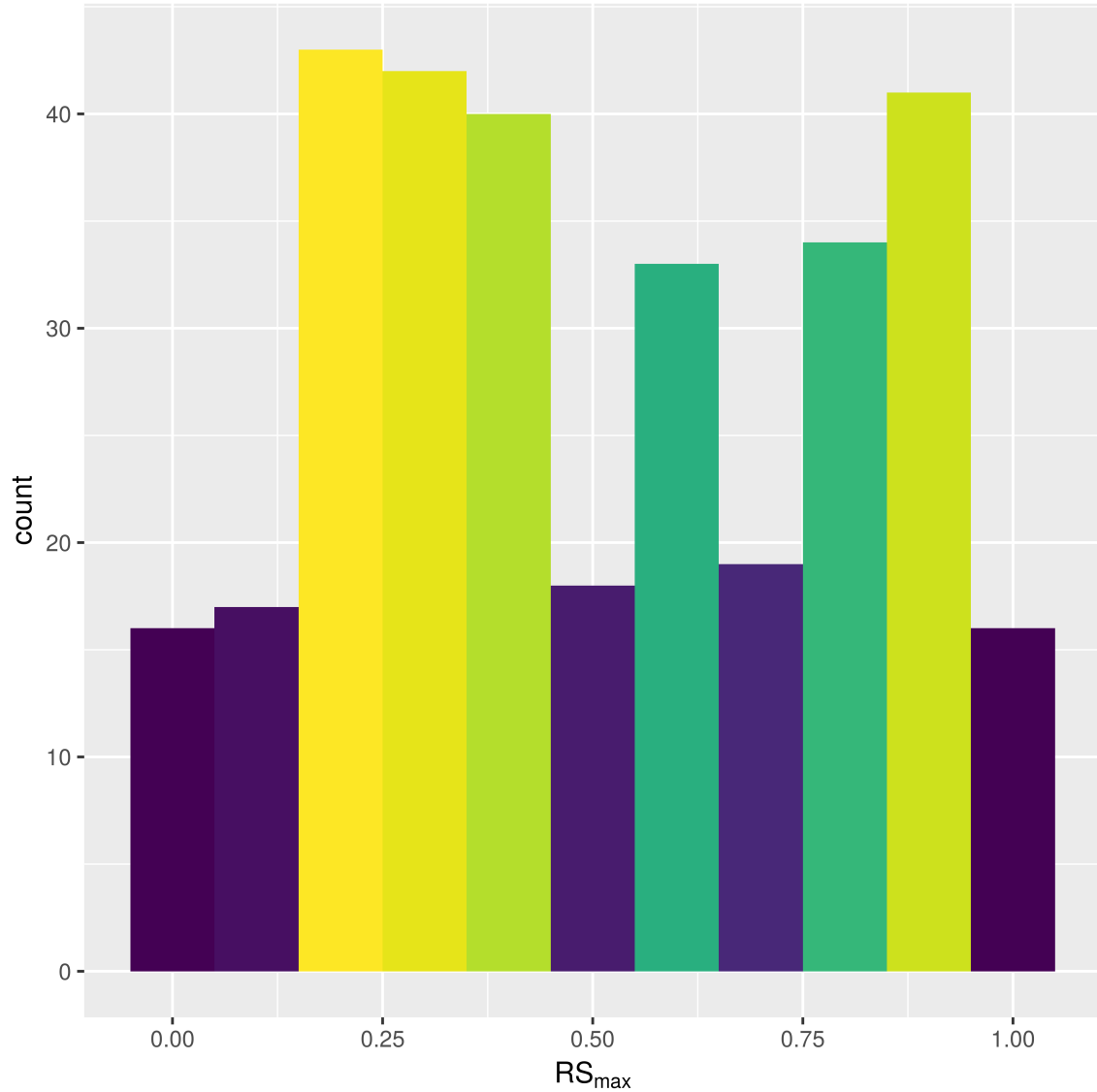


Figure 3: Frequency distribution of Largest patch proportion relative to total forest area RS_{max} calculated using a threshold of 40% of forest in each pixel to determine patches. Bimodality is observed and confirmed by the dip test ($D = 0.0416$, $p\text{-value} = 0.0003$). This indicates the existence of two states needed for a critical transition.

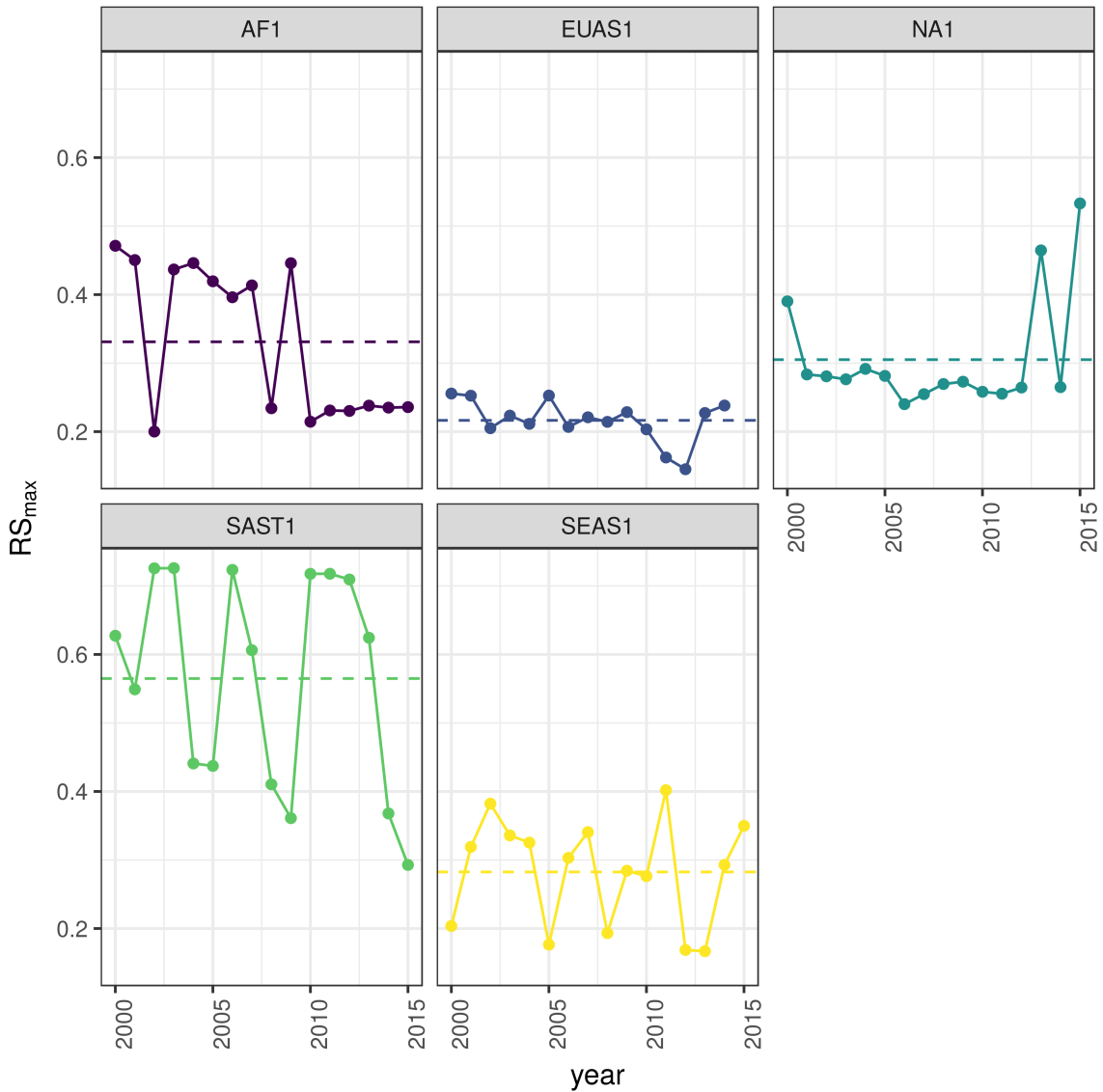


Figure 4: Largest patch proportion relative to total forest area RS_{max} , for regions with total forest area $> 10^7 \text{ km}^2$. We show here the RS_{max} calculated using a threshold of 40% of forest in each pixel to determine patches. Dashed lines are averages across time. The regions are AF1: Africa mainland, EUAS1: Eurasia mainland, NA1: North America mainland, SAST1: South America tropical and subtropical, SEAS1: Southeast Asia mainland.

304 with confidence which is the best distribution. Only 1 case the distribution selected by the Akaike criteria is
305 confirmed as the correct model for relative and absolute fluctuations (Table S4). Thus we do not apply this
306 criteria because is not informative, we can not decide with reliability if the best distribution is the selected
307 one.

308 The animations of the two largest patches (see supplementary data, largest patch gif animations) qualitatively
309 shows the nature of fluctuations and if the state of the forest is connected or not. If the largest patch is
310 always the same patch over time, the forest is probably not fragmented; this happens for regions with RS_{max}
311 of more than 40% such as AF2 (Madagascar), EUAS2 (Japan), NA5 (Newfoundland) and OC3 (Malaysia).
312 In the regions with RS_{max} between 40% and 30% the identity of the largest patch could change or stay the
313 same in time. For OC7 (Java) the largest patch changes and for AF1 (Africa mainland) it stays the same.
314 Only for EUAS1 (Eurasia mainland) we observed that the two largest patches are always the same, implying
315 that this region is probably composed of two independent domains and should be divided in further studies.
316 The regions with RS_{max} less than 25%: SAST2 (Cuba) and EUAS3 (Great Britain), the largest patch always
317 changes reflecting their fragmented state. In the case of SEAS2 (Philippines) a transition is observed, with
318 the identity of the largest patch first variable, and then constant after 2010.

319 The results of quantile regressions are almost identical for ΔRS_{max} and ΔS_{max} (table S5); in very few cases
320 only one of them is significant but we only take into account results where both are significant. Among
321 the biggest regions, Africa (AF1) has a similar pattern across thresholds but only at 30% is significant; the
322 upper and lower quantiles have significant negative slopes, but the lower quantile slope is lower, implying
323 that negative fluctuations and variance are increasing (Figure 5). Eurasia mainland (EUAS1) has significant
324 slopes at 20%, 30% and 40% thresholds but the patterns are different at 20% variance is decreasing, at 30%
325 and 40% only is increasing. This is because the largest patch is composed of pixels with different cover of
326 forest, thus there are more variation in pixels from 30% to 20% than from 20% to less than 20%, then the
327 fluctuations are happening between 40% and 20%. The signal is that the variation of the most dense portion
328 of the largest patch is increasing. North America mainland (NA1) exhibits the same pattern at 20%, 25%
329 and 30% thresholds: a significant lower quantile with positive slope, implying decreasing variance. South
330 America tropical and subtropical (SAST1) have significant lower quantile with negative slope at 25% and
331 30% thresholds indicating an increase in variance. Finally, SEAS1 have a upper quantile with positive slope
332 significant for 25% threshold, also indicating an increasing variance. The plots for other regions are showed
333 in the appendix (Figures Sx - Sx) and all these results are summarized in Table 1.

334 The conditions that indicate that a region is near a critical fragmentation threshold are that patch size
335 distributions follow a power law; temporal ΔRS_{max} fluctuations follow a power law; variance of ΔRS_{max} is

336 increasing in time; and skewness is negative. All these conditions were true only for Africa mainland (AF1)
 337 and South America tropical & subtropical (SAST1).

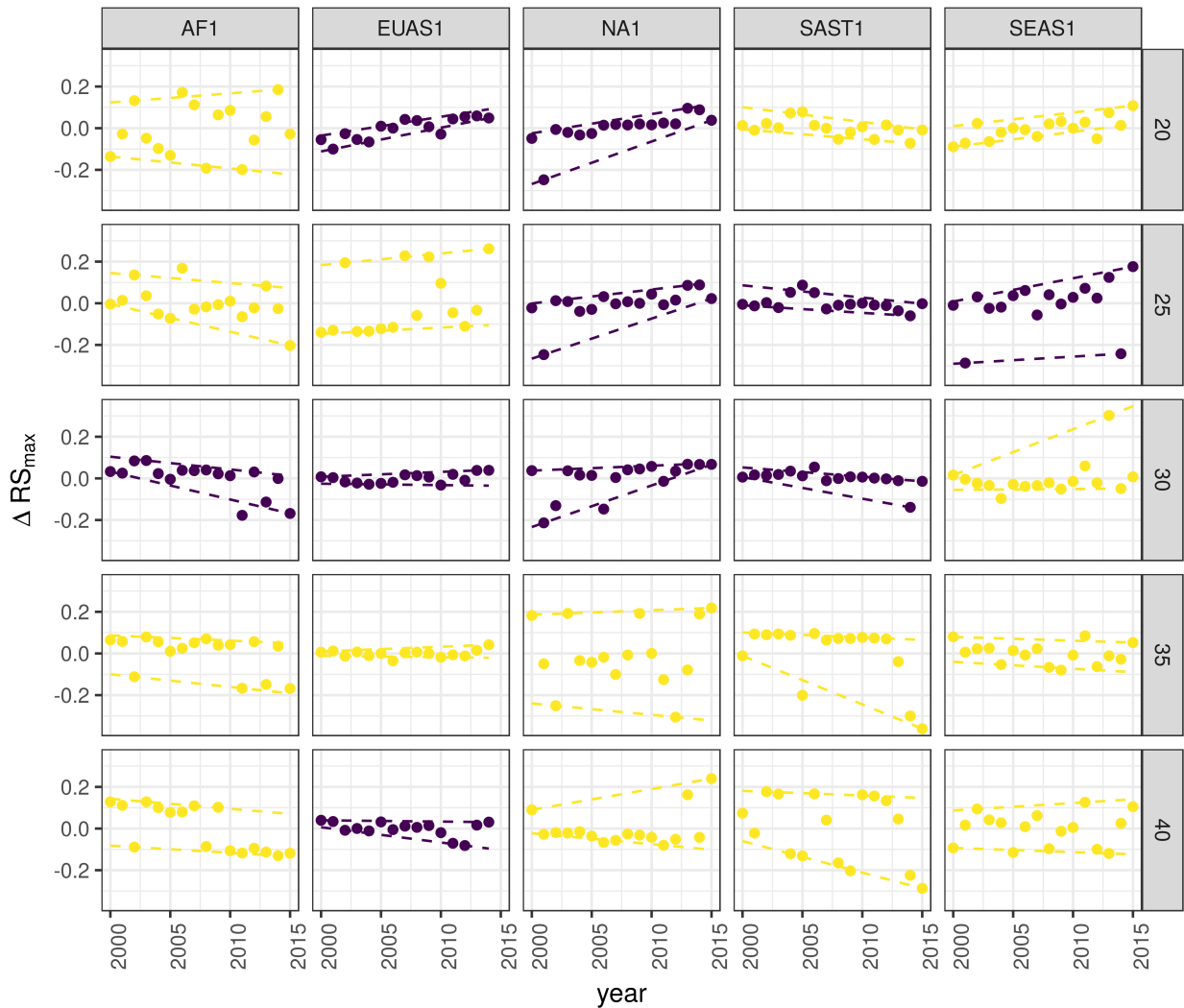


Figure 5: Largest patch fluctuations for regions with total forest area $> 10^7 \text{ km}^2$ across years. The patch sizes are relative to the total forest area of the same year. Dashed lines are 90% and 10% quantile regressions, to show if fluctuations were increasing; purple (dark) panels have significant slopes. The regions are AF1: Africa mainland, EUAS1: Eurasia mainland, NA1: North America mainland, SAST1: South America tropical and subtropical, SEAS1: Southeast Asia mainland.

Table 1: Regions and indicators of closeness to a critical fragmentation point. Where: RS_{max} is the largest patch divided by the total forest area; Threshold is the value used to calculate patches from the MODIS VCF pixels; ΔRS_{max} are the fluctuations of RS_{max} around the mean and the increase or decrease in the variance was estimated using quantile regressions; skewness was calculated for RS_{max} . NS means the results were non-significant. The conditions that determine the closeness to a fragmentation point are: increasing variance of ΔRS_{max} and negative skewness. RS_{max} indicates if the forest is unfragmented (>0.6) or fragmented (<0.3).

Region	Description	Variance of			
		RS_{max}	Threshold	ΔRS_{max}	Skewness
AF1	Africa mainland	0.33	30	Increase	-1.4653
AF2	Madagascar	0.48	20	Increase	0.7226
EUAS1	Eurasia, mainland	0.22	20	Decrease	-0.4814
EUAS1			30	Increase	0.3113
EUAS1			40	Increase	-1.2790
EUAS2	Japan	0.94	35	Increase	-0.3913
EUAS2			40	Increase	-0.5030
EUAS3	Great Britain	0.03	40	NS	
NA1	North America, mainland	0.31	20	Decrease	-2.2895
NA1			25	Decrease	-2.4465
NA1			30	Decrease	-1.6340
NA5	Newfoundland	0.54	40	NS	
OC1	Australia, Mainland	0.36	30	Increase	0.0920
OC1			35	Increase	-0.8033
OC2	New Guinea	0.96	25	Decrease	-0.1003
OC2			30	Decrease	0.1214
OC2			35	Decrease	-0.0124
OC3	Malaysia/Kalimantan	0.92	35	Increase	-1.0147
OC3			40	Increase	-1.5649
OC4	Sumatra	0.84	20	Increase	-1.3846
OC4			25	Increase	-0.5887
OC4			30	Increase	-1.4226
OC5	Sulawesi	0.82	40	NS	
OC6	New Zealand South Island	0.75	40	Increase	0.3553
OC7	Java	0.16	40	NS	

Region	Description	RS_{max}	Threshold	Variance of	
				ΔRS_{max}	Skewness
OC8	New Zealand North Island	0.64	40	NS	
SAST1	South America, Tropical and Subtropical forest up to Mexico	0.56	25	Increase	1.0519
SAST1			30	Increase	-2.7216
SAST2	Cuba	0.15	20	Increase	0.5049
SAST2			25	Increase	1.7263
SAST2			30	Increase	0.1665
SAST2			40	Increase	-0.5401
SAT1	South America, Temperate forest	0.54	25	Decrease	0.1483
SAT1			30	Decrease	-1.6059
SAT1			35	Decrease	-1.3809
SEAS1	Southeast Asia, Mainland	0.28	25	Increase	-1.3328
SEAS2	Philippines	0.33	20	Decrease	-1.6373
SEAS2			25	Decrease	-0.6648
SEAS2			30	Increase	0.1517
SEAS2			40	Increase	1.5996

338 Discussion

339 We found that the forest patch distribution of most regions of the world followed power laws spanning
 340 seven orders of magnitude. These include tropical rainforest, boreal and temperate forest. Power laws have
 341 previously been found for several kinds of vegetation, but never at global scales as in this study. Interestingly,
 342 Eurasia does not follow a power law, but it is a geographically extended region, consisting of different domains
 343 (as we observed in the largest patch animations, see supplementary data). It is known that the union of two
 344 independent power law distributions produces a lognormal distribution (Rooij et al., 2013). Future studies
 345 should split this region into two or more new regions, and test if the underlying distributions are power laws.
 346 Several mechanisms have been proposed for the emergence of power laws in forest: the first is related self

organized criticality (SOC), when the system is driven by its internal dynamics to a critical state; this has been suggested mainly for fire-driven forests (Hantson, Pueyo, & Chuvieco, 2015; Zinck & Grimm, 2009). Real ecosystems do not seem to meet the requirements of SOC dynamics (McKenzie & Kennedy, 2012; S. Pueyo et al., 2010; Sole, Alonso, & Mckane, 2002). A second possible mechanism, suggested by Pueyo et al. (2010), is isotropic percolation, when a system is near the critical point power law structures arise. This is equivalent to the random forest model that we explained previously, and requires the tuning of an external environmental condition to carry the system to this point. We did not expect forest growth to be a random process at local scales, but it is possible that combinations of factors cancel out to produce seemingly random forest dynamics at large scales. If this is the case the power law exponent should be theoretically near $\alpha = 2.055$; this is close but outside the confidence interval we observed (1.898 - 1.920). The third mechanism suggested as the cause of pervasive power laws in patch size distribution is facilitation (Irvine, Bull, & Keeling, 2016; Manor & Shnerb, 2008): a patch surrounded by forest will have a smaller probability of been deforested or degraded than an isolated patch. We hypothesize that models that include facilitation could explain the patterns observed here. The model of Scanlon et al. (2007) showed an $\alpha = 1.34$ which is also different from our results. Another model but with three states (tree/non-tree/degraded), including local facilitation and grazing, was also used to obtain power laws patch distributions without external tuning, and exhibited deviations from power laws at high grazing pressures (S. Kéfi et al., 2007). The values of the power law exponent α obtained for this model are dependent on the intensity of facilitation, when facilitation is more intense the exponent is higher, but the maximal values they obtained are still lower than the ones we observed. The interesting point is that the value of the exponent is dependent on the parameters, and thus the observed α might be obtained with some parameter combination.

It has been suggested that a combination of spatial and temporal indicators could more reliably detect critical transitions (S. Kéfi et al., 2014). In this study, we combined five criteria to detect the closeness to a fragmentation threshold. Two of them were spatial: the forest patch size distribution, and the proportion of the largest patch relative to total forest area (RS_{max}). The other three were the distribution of temporal fluctuations in the largest patch size, the trend in the variance, and the skewness of the fluctuations. Each one of these is not a strong individual predictor, but their combination gives us an increased degree of confidence about the system being close to a critical transition.

We found that only the tropical forest of Africa and South America met all five criteria, and thus seem to be near a critical fragmentation threshold. This confirms previous studies that point to these two tropical areas as the most affected by deforestation (M. C. Hansen et al., 2013). Africa seems to be more affected, because the proportion of the largest patch relative to total forest area (RS_{max}) is near 30%, which could indicate

379 that the transition is already started. Moreover, this region was estimated to be potentially bistable, with
380 the possibility to completely transform into a savanna (Staver, Archibald, & Levin, 2011). The main driver
381 of deforestation in this area was smallholder farming.

382 The region of South America tropical forest has a RS_{max} of more than 60%, suggesting that the fragmentation
383 transition is approaching but not yet started. In this region, a striking decline in deforestation rates has
384 been observed in Brasil, which hosts most of the biggest forest patch, but deforestation rates have continued
385 to increase in surrounding countries (Argentina, Paraguay, Bolivia, Colombia, Peru) thus the region is still
386 at a high risk.

387 The monitoring of biggest patches is also important because they contain most of the intact forest landscapes
388 defined by P. Potapov et al. (2008), thus a relatively simple way to evaluate the risk in these areas is to
389 use RS_{max} index. The analysis of RS_{max} reveals that the island of Philippines (SEAS2) seems to be an
390 example of a critical transition from an unconnected to a connected state, the early warning signals can
391 be qualitatively observed: a big fluctuation in a negative direction precedes the transition and then RS_{max}
392 stabilizes over 60% (Figure S9). In addition, there was a total loss of forest cover of 1.9% from year 2000 to
393 2012 (M. C. Hansen et al., 2013) and deforestation rates were not substantially reduced in 1990-2014; this
394 could be the results of an active intervention of the government promoting conservation and rehabilitation
395 of protected areas, ban of logging old-growth forest, reforestation of barren areas, community-based forestry
396 activities, and sustainable forest management in the country's production forest (Lasco et al., 2008). This
397 confirms that the early warning indicators proposed here work in the correct direction.

398 The region of Southeast Asia was also one of the most deforested places in the world, but was not detected
399 as a region near a fragmentation threshold. This is probably due to the forest conservation and restoration
400 programs implemented by the Chinese government, which bans logging in natural forests and monitor illegal
401 harvesting (Viña, McConnell, Yang, Xu, & Liu, 2016). The MODIS dataset does not detect if native forest
402 is replaced by agroindustrial tree plantations like oil palms, that are among the main drivers of deforestation
403 in this area (Malhi, Gardner, Goldsmith, Silman, & Zelazowski, 2014). To improve the estimation of forest
404 patches, data sets as the MODIS cropland probability and others about land use, protected areas, forest
405 type, should be incorporated (M. Hansen et al., 2014; J. O. Sexton et al., 2015).

406 Deforestation and fragmentation are closely related. At low levels of habitat reduction species population
407 will decline proportionally; this can happen even when the habitat fragments retain connectivity. As habi-
408 tat reduction continues, the critical threshold is approached and connectivity will have large fluctuations
409 (Brook, Ellis, Perring, Mackay, & Blomqvist, 2013). This could trigger several negative synergistic effects:

410 populations fluctuations and the possibility of extinctions will rise, increasing patch isolation and decreasing
411 connectivity (Brook et al., 2013). This positive feedback mechanism will be enhanced when the fragmenta-
412 tion threshold is reached, resulting in the loss of most habitat specialist species at a landscape scale (Pardini
413 et al., 2010). Some authors argue that since species have heterogeneous responses to habitat loss and frag-
414 mentation, and biotic dispersal is limited, the importance of thresholds is restricted to local scales or even
415 that its existence is questionable (Brook et al., 2013). Fragmentation is by definition a local process that at
416 some point produces emergent phenomena over the entire landscape, even if the area considered is infinite
417 (B. Oborny, Meszéna, & Szabó, 2005). In addition, after a region's fragmentation threshold connectivity
418 decreases, there is still a large and internally well connected patch that can maintain sensitive species (A. C.
419 Martensen, Ribeiro, Banks-Leite, Prado, & Metzger, 2012). What is the time needed for these large patches
420 to become fragmented, and pose a real danger of extinction to a myriad of sensitive species? If a forest is
421 already in a fragmented state, a second critical transition from forest to non-forest could happen, this was
422 called the desertification transition (Corrado et al., 2014). Considering the actual trends of habitat loss,
423 and studying the dynamics of non-forest patches—instead of the forest patches as we did here—the risk of
424 this kind of transition could be estimated. The simple models proposed previously could also be used to
425 estimate if these thresholds are likely to be continuous and reversible or discontinuous and often irreversible
426 (Weissmann & Shnerb, 2016), and the degree of protection (e.g. using the set-asides strategy Banks-Leite et
427 al. (2014)) than would be necessary to stop this trend.

428 The effectiveness of landscape management is related to the degree of fragmentation, and the criteria to
429 direct reforestation efforts could be focused on regions near a transition (B. Oborny et al., 2007). Regions
430 that are in an unconnected state require large efforts to recover a connected state, but regions that are near
431 a transition could be easily pushed to a connected state; feedbacks due to facilitation mechanisms might
432 help to maintain this state. Crossing the fragmentation critical point in forests could have negative effects
433 on biodiversity and ecosystem services (Haddad et al., 2015), but it could also produce feedback loops at
434 different levels of the biological hierarchy. This means that a critical transition produced at a continental
435 scale could have effects at the level of communities, food webs, populations, phenotypes and genotypes
436 (Barnosky et al., 2012). All these effects interact with climate change, thus there is a potential production of
437 cascading effects that could lead to a global collapse. Therefore, even if critical thresholds are reached only in
438 some forest regions at a continental scale, a cascading effect with global consequences could still be produced,
439 and may contribute to reach a planetary tipping point (Reyer, Rammig, Brouwers, & Langerwisch, 2015).
440 The risk of such event will be higher if the dynamics of separate continental regions are coupled (Lenton &
441 Williams, 2013). Using the time series obtained in this work the coupling of the continental could be further

442 investigated. It has been proposed that to assess the probability of a global scale shift, different small scale
443 ecosystems should be studied in parallel (Barnosky et al., 2012). As forest comprises a major proportion
444 of such ecosystems, we think that the transition of forests could be used as a proxy for all the underlying
445 changes and as a successful predictor of a planetary tipping point.

446 **Supporting information**

447 **Appendix**

448 *Table S1:* Proportion of Power law models not rejected by the goodness of fit test at $p \leq 0.05$ level.

449 *Table S2:* Generalized least squares fit by maximizing the restricted log-likelihood.

450 *Table S3:* Simultaneous Tests for General Linear Hypotheses of the power law exponent.

451 *Table S4:* Quantile regressions of the proportion of largest patch area vs year.

452 *Table S5:* Unbiased estimation of skewness for absolute largest patch fluctuations and relative fluctuations.

453 *Table S6:* Model selection using Akaike criterion for largest patch fluctuations in absolute values

454 *Table S7:* Model selection for fluctuation of largest patch in relative to total forest area.

455 *Figure S1:* Regions for Africa (AF), 1 Mainland, 2 Madagascar.

456 *Figure S2:* Regions for Eurasia (EUAS), 1 Mainland, 2 Japan, 3 Great Britain.

457 *Figure S3:* Regions for North America (NA), 1 Mainland, 5 Newfoundland.

458 *Figure S4:* Regions for Australia and islands (OC), 1 Australia mainland; 2 New Guinea; 3 Malaysia/Kalimantan;
459 4 Sumatra; 5 Sulawesi; 6 New Zealand south island; 7 Java; 8 New Zealand north island.

460 *Figure S5:* Regions for South America, SAST1 Tropical and subtropical forest up to Mexico; SAST2 Cuba;
461 SAT1 South America, Temperate forest.

462 *Figure S6:* Regions for Southeast Asia (SEAS), 1 Mainland; 2 Philippines.

463 *Figure S7:* Proportion of best models selected for patch size distributions using the Akaike criterion.

464 *Figure S8:* Power law exponents for forest patch distributions by year.

465 *Figure S9:* Largest patch proportion relative to total forest area RS_{max} , for regions with total forest area
466 less than 10^7 km^2 .

⁴⁶⁷ *Figure S10:* Fluctuations of largest patch for regions with total forest area less than 10^7 km². The patch
⁴⁶⁸ sizes are relativized to the total forest area for that year.

⁴⁶⁹ Data Accessibility

⁴⁷⁰ Csv text file with model fits for patch size distribution, and model selection for all the regions; Gif Animations
⁴⁷¹ of a forest model percolation; Gif animations of largest patches; patch size files for all years and regions
⁴⁷² used here; and all the R and Matlab scripts are available at figshare <http://dx.doi.org/10.6084/m9.figshare.4263905>.

⁴⁷⁴ Acknowledgments

⁴⁷⁵ LAS and SRD are grateful to the National University of General Sarmiento for financial support. This work
⁴⁷⁶ was partially supported by a grant from CONICET (PIO 144-20140100035-CO).

⁴⁷⁷ References

- ⁴⁷⁸ Allington, G. R. H., & Valone, T. J. (2010). Reversal of desertification: The role of physical and chemical
⁴⁷⁹ soil properties. *Journal of Arid Environments*, 74(8), 973–977. doi:10.1016/j.jaridenv.2009.12.005
- ⁴⁸⁰ Alstott, J., Bullmore, E., & Plenz, D. (2014). powerlaw: A Python Package for Analysis of Heavy-Tailed
⁴⁸¹ Distributions. *PLOS ONE*, 9(1), e85777. Retrieved from <https://doi.org/10.1371/journal.pone.0085777>
- ⁴⁸² Banks-Leite, C., Pardini, R., Tambosi, L. R., Pearse, W. D., Bueno, A. A., Bruscagin, R. T., ... Metzger,
⁴⁸³ J. P. (2014). Using ecological thresholds to evaluate the costs and benefits of set-asides in a biodiversity
⁴⁸⁴ hotspot. *Science*, 345(6200), 1041–1045. doi:10.1126/science.1255768
- ⁴⁸⁵ Barnosky, A. D., Hadly, E. A., Bascompte, J., Berlow, E. L., Brown, J. H., Fortelius, M., ... Smith, A. B.
⁴⁸⁶ (2012). Approaching a state shift in Earth’s biosphere. *Nature*, 486(7401), 52–58. doi:10.1038/nature11018
- ⁴⁸⁷ Bascompte, J., & Solé, R. V. (1996). Habitat fragmentation and extinction thresholds in spatially explicit
⁴⁸⁸ models. *Journal of Animal Ecology*, 65(4), 465–473. doi:10.2307/5781
- ⁴⁸⁹ Bazant, M. Z. (2000). Largest cluster in subcritical percolation. *Physical Review E*, 62(2), 1660–1669.
⁴⁹⁰ Retrieved from <http://link.aps.org/doi/10.1103/PhysRevE.62.1660>
- ⁴⁹¹ Belward, A. S. (1996). *The IGBP-DIS Global 1 Km Land Cover Data Set “DISCover”: Proposal and*

- ⁴⁹² *Implementation Plans : Report of the Land Recover Working Group of IGBP-DIS* (p. 61). IGBP-DIS Office.
- ⁴⁹³ Retrieved from <https://books.google.com.ar/books?id=qixsNAAACAAJ>
- ⁴⁹⁴ Benedetti-Cecchi, L., Tamburello, L., Maggi, E., & Bulleri, F. (2015). Experimental Perturbations Modify the Performance of Early Warning Indicators of Regime Shift. *Current Biology*, 25(14), 1867–1872.
- ⁴⁹⁵
- ⁴⁹⁶ doi:10.1016/j.cub.2015.05.035
- ⁴⁹⁷ Bestelmeyer, B. T., Duniway, M. C., James, D. K., Burkett, L. M., & Havstad, K. M. (2013). A test of critical thresholds and their indicators in a desertification-prone ecosystem: more resilience than we thought.
- ⁴⁹⁸
- ⁴⁹⁹ *Ecology Letters*, 16, 339–345. doi:10.1111/ele.12045
- ⁵⁰⁰ Bestelmeyer, B. T., Ellison, A. M., Fraser, W. R., Gorman, K. B., Holbrook, S. J., Laney, C. M., ... Sharma, S. (2011). Analysis of abrupt transitions in ecological systems. *Ecosphere*, 2(12), 129. doi:10.1890/ES11-00216.1
- ⁵⁰¹
- ⁵⁰²
- ⁵⁰³ Boettiger, C., & Hastings, A. (2012). Quantifying limits to detection of early warning for critical transitions.
- ⁵⁰⁴ *Journal of the Royal Society Interface*, 9(75), 2527–2539. doi:10.1098/rsif.2012.0125
- ⁵⁰⁵ Bonan, G. B. (2008). Forests and Climate Change: forcings, Feedbacks, and the Climate Benefits of Forests.
- ⁵⁰⁶ *Science*, 320(5882), 1444–1449. doi:10.1126/science.1155121
- ⁵⁰⁷ Botet, R., & Ploszajczak, M. (2004). Correlations in Finite Systems and Their Universal Scaling Properties.
- ⁵⁰⁸ In K. Morawetz (Ed.), *Nonequilibrium physics at short time scales: Formation of correlations* (pp. 445–466).
- ⁵⁰⁹ Berlin Heidelberg: Springer-Verlag.
- ⁵¹⁰ Brook, B. W., Ellis, E. C., Perring, M. P., Mackay, A. W., & Blomqvist, L. (2013). Does the terrestrial
- ⁵¹¹ biosphere have planetary tipping points? *Trends in Ecology & Evolution*. doi:10.1016/j.tree.2013.01.016
- ⁵¹² Burnham, K., & Anderson, D. R. (2002). *Model selection and multi-model inference: A practical information-theoretic approach* (2nd. ed., p. 512). New York: Springer-Verlag.
- ⁵¹³
- ⁵¹⁴ Canfield, D. E., Glazer, A. N., & Falkowski, P. G. (2010). The Evolution and Future of Earth's Nitrogen
- ⁵¹⁵ Cycle. *Science*, 330(6001), 192–196. doi:10.1126/science.1186120
- ⁵¹⁶ Carpenter, S. R., Cole, J. J., Pace, M. L., Batt, R., Brock, W. A., Cline, T., ... Weidel, B. (2011).
- ⁵¹⁷ Early Warnings of Regime Shifts: A Whole-Ecosystem Experiment. *Science*, 332(6033), 1079–1082.
- ⁵¹⁸ doi:10.1126/science.1203672
- ⁵¹⁹ Clauset, A., Shalizi, C., & Newman, M. (2009). Power-Law Distributions in Empirical Data. *SIAM Review*,

- 520 51(4), 661–703. doi:10.1137/070710111
- 521 Corrado, R., Cherubini, A. M., & Pennetta, C. (2014). Early warning signals of desertification transitions
522 in semiarid ecosystems. *Physical Review E - Statistical, Nonlinear, and Soft Matter Physics*, 90(6), 62705.
523 doi:10.1103/PhysRevE.90.062705
- 524 Crawley, M. J. (2012). *The R Book* (2nd. ed., p. 1076). Hoboken, NJ, USA: Wiley.
- 525 Crowther, T. W., Glick, H. B., Covey, K. R., Bettigole, C., Maynard, D. S., Thomas, S. M., ... Bradford, M.
526 A. (2015). Mapping tree density at a global scale. *Nature*, 525(7568), 201–205. doi:10.1038/nature14967
- 527 Dai, L., Vorselen, D., Korolev, K. S., & Gore, J. (2012). Generic Indicators for Loss of Resilience Before a
528 Tipping Point Leading to Population Collapse. *Science*, 336(6085), 1175–1177. doi:10.1126/science.1219805
- 529 DiMiceli, C., Carroll, M., Sohlberg, R., Huang, C., Hansen, M., & Townshend, J. (2015). Annual Global Au-
530 tomated MODIS Vegetation Continuous Fields (MOD44B) at 250 m Spatial Resolution for Data Years Begin-
531 ning Day 65, 2000 - 2014, Collection 051 Percent Tree Cover, University of Maryland, College Park, MD, USA.
532 Retrieved from https://lpdaac.usgs.gov/dataset{_}discovery/modis/modis{_}products{_}table/mod44b
- 533 Drake, J. M., & Griffen, B. D. (2010). Early warning signals of extinction in deteriorating environments.
534 *Nature*, 467(7314), 456–459. doi:10.1038/nature09389
- 535 Efron, B., & Tibshirani, R. J. (1994). *An Introduction to the Bootstrap* (p. 456). New York: Taylor &
536 Francis. Retrieved from <https://books.google.es/books?id=gLlpIUXRntoC>
- 537 Filotas, E., Parrott, L., Burton, P. J., Chazdon, R. L., Coates, K. D., Coll, L., ... Messier, C. (2014). Viewing
538 forests through the lens of complex systems science. *Ecosphere*, 5(January), 1–23. doi:10.1890/ES13-00182.1
- 539 Foley, J. A., Ramankutty, N., Brauman, K. A., Cassidy, E. S., Gerber, J. S., Johnston, M., ... Zaks, D. P. M.
540 (2011). Solutions for a cultivated planet. *Nature*, 478(7369), 337–342. doi:10.1038/nature10452
- 541 Folke, C., Jansson, Å., Rockström, J., Olsson, P., Carpenter, S. R., Iii, F. S. C., ... Westley, F. (2011).
542 Reconnecting to the Biosphere. *AMBIO*, 40(7), 719–738. doi:10.1007/s13280-011-0184-y
- 543 Fung, T., O'Dwyer, J. P., Rahman, K. A., Fletcher, C. D., & Chisholm, R. A. (2016). Reproducing static
544 and dynamic biodiversity patterns in tropical forests: the critical role of environmental variance. *Ecology*,
545 97(5), 1207–1217. doi:10.1890/15-0984.1
- 546 Gardner, R. H., & Urban, D. L. (2007). Neutral models for testing landscape hypotheses. *Landscape Ecology*,
547 22(1), 15–29. doi:10.1007/s10980-006-9011-4
- 548 Gastner, M. T., Oborny, B., Zimmermann, D. K., & Pruessner, G. (2009). Transition from Connected

- 549 to Fragmented Vegetation across an Environmental Gradient: Scaling Laws in Ecotone Geometry. *The*
550 *American Naturalist*, 174(1), E23–E39. doi:10.1086/599292
- 551 Gilman, S. E., Urban, M. C., Tewksbury, J., Gilchrist, G. W., & Holt, R. D. (2010). A framework
552 for community interactions under climate change. *Trends in Ecology & Evolution*, 25(6), 325–331.
553 doi:10.1016/j.tree.2010.03.002
- 554 Goldstein, M. L., Morris, S. A., & Yen, G. G. (2004). Problems with fitting to the power-law distri-
555 bution. *The European Physical Journal B - Condensed Matter and Complex Systems*, 41(2), 255–258.
556 doi:10.1140/epjb/e2004-00316-5
- 557 Haddad, N. M., Brudvig, L. a., Clobert, J., Davies, K. F., Gonzalez, A., Holt, R. D., ... Townshend, J. R.
558 (2015). Habitat fragmentation and its lasting impact on Earth's ecosystems. *Science Advances*, 1(2), 1–9.
559 doi:10.1126/sciadv.1500052
- 560 Hansen, M. C., Potapov, P. V., Moore, R., Hancher, M., Turubanova, S. A., Tyukavina, A., ... Townshend,
561 J. R. G. (2013). High-Resolution Global Maps of 21st-Century Forest Cover Change. *Science*, 342(6160),
562 850–853. doi:10.1126/science.1244693
- 563 Hansen, M., Potapov, P., Margono, B., Stehman, S., Turubanova, S., & Tyukavina, A. (2014). Response
564 to Comment on “High-resolution global maps of 21st-century forest cover change”. *Science*, 344(6187), 981.
565 doi:10.1126/science.1248817
- 566 Hantson, S., Pueyo, S., & Chuvieco, E. (2015). Global fire size distribution is driven by human impact and
567 climate. *Global Ecology and Biogeography*, 24(1), 77–86. doi:10.1111/geb.12246
- 568 Harris, T. E. (1974). Contact interactions on a lattice. *The Annals of Probability*, 2, 969–988.
- 569 Hartigan, J. A., & Hartigan, P. M. (1985). The Dip Test of Unimodality. *The Annals of Statistics*, 13(1),
570 70–84. Retrieved from <http://www.jstor.org/stable/2241144>
- 571 Hastings, A., & Wysham, D. B. (2010). Regime shifts in ecological systems can occur with no warning.
572 *Ecology Letters*, 13(4), 464–472. doi:10.1111/j.1461-0248.2010.01439.x
- 573 He, F., & Hubbell, S. (2003). Percolation Theory for the Distribution and Abundance of Species. *Physical*
574 *Review Letters*, 91(19), 198103. doi:10.1103/PhysRevLett.91.198103
- 575 Hinrichsen, H. (2000). Non-equilibrium critical phenomena and phase transitions into absorbing states.
576 *Advances in Physics*, 49(7), 815–958. doi:10.1080/00018730050198152
- 577 Hirota, M., Holmgren, M., Nes, E. H. V., & Scheffer, M. (2011). Global Resilience of Tropical Forest and

- 578 Savanna to Critical Transitions. *Science*, 334(6053), 232–235. doi:10.1126/science.1210657
- 579 Irvine, M. A., Bull, J. C., & Keeling, M. J. (2016). Aggregation dynamics explain vegetation patch-size
580 distributions. *Theoretical Population Biology*, 108, 70–74. doi:10.1016/j.tpb.2015.12.001
- 581 Keitt, T. H., Urban, D. L., & Milne, B. T. (1997). Detecting critical scales in fragmented landscapes.
582 *Conservation Ecology*, 1(1), 4. Retrieved from <http://www.ecologyandsociety.org/vol1/iss1/art4/>
- 583 Kéfi, S., Guttal, V., Brock, W. A., Carpenter, S. R., Ellison, A. M., Livina, V. N., ... Dakos, V. (2014).
584 Early Warning Signals of Ecological Transitions: Methods for Spatial Patterns. *PLoS ONE*, 9(3), e92097.
585 doi:10.1371/journal.pone.0092097
- 586 Kéfi, S., Rietkerk, M., Alados, C. L., Pueyo, Y., Papanastasis, V. P., ElAich, A., & Ruiter, P. C. de.
587 (2007). Spatial vegetation patterns and imminent desertification in Mediterranean arid ecosystems. *Nature*,
588 449(7159), 213–217. doi:10.1038/nature06111
- 589 Kitzberger, T., Aráoz, E., Gowda, J. H., Mermoz, M., & Morales, J. M. (2012). Decreases in Fire Spread
590 Probability with Forest Age Promotes Alternative Community States, Reduced Resilience to Climate Vari-
591 ability and Large Fire Regime Shifts. *Ecosystems*, 15(1), 97–112. doi:10.1007/s10021-011-9494-y
- 592 Koenker, R. (2016). quantreg: Quantile Regression. Retrieved from <http://cran.r-project.org/package=quantreg>
- 594 Lasco, R. D., Pulhin, F. B., Cruz, R. V. O., Pulhin, J. M., Roy, S. S. N., & Sanchez, P. A. J. (2008). Forest
595 responses to changing rainfall in the Philippines. In N. Leary, C. Conde, & J. Kulkarni (Eds.), *Climate
596 change and vulnerability* (pp. 49–66). London: Earthscan. Retrieved from <http://gen.lib.rus.ec/book/index.php?md5=AD313B13E05C9D61A9EC1EE2E73A91FB>
- 598 Leibold, M. A., & Norberg, J. (2004). Biodiversity in metacommunities: Plankton as complex adaptive
599 systems? *Limnology and Oceanography*, 49(4, part 2), 1278–1289. doi:10.4319/lo.2004.49.4_part_2.1278
- 600 Lenton, T. M., & Williams, H. T. P. (2013). On the origin of planetary-scale tipping points. *Trends in
601 Ecology & Evolution*, 28(7), 380–382. doi:10.1016/j.tree.2013.06.001
- 602 Limpert, E., Stahel, W. A., & Abbt, M. (2001). Log-normal Distributions across the Sciences: Keys and
603 CluesOn the charms of statistics, and how mechanical models resembling gambling machines offer a link to
604 a handy way to characterize log-normal distributions, which can provide deeper insight into var. *BioScience*,
605 51(5), 341–352. Retrieved from [http://dx.doi.org/10.1641/0006-3568\(2001\)051\[0341:LNDATS\]2.0.CO](http://dx.doi.org/10.1641/0006-3568(2001)051[0341:LNDATS]2.0.CO)
- 606 Loehle, C., Li, B.-L., & Sundell, R. C. (1996). Forest spread and phase transitions at forest-prairie ecotones

- 607 in Kansas, U.S.A. *Landscape Ecology*, 11(4), 225–235.
- 608 Malhi, Y., Gardner, T. A., Goldsmith, G. R., Silman, M. R., & Zelazowski, P. (2014). Tropical Forests in
609 the Anthropocene. *Annual Review of Environment and Resources*, 39(1), 125–159. doi:10.1146/annurev-
610 environ-030713-155141
- 611 Manor, A., & Shnerb, N. M. (2008). Origin of pareto-like spatial distributions in ecosystems. *Physical*
612 *Review Letters*, 101(26), 268104. doi:10.1103/PhysRevLett.101.268104
- 613 Martensen, A. C., Ribeiro, M. C., Banks-Leite, C., Prado, P. I., & Metzger, J. P. (2012). Associations
614 of Forest Cover, Fragment Area, and Connectivity with Neotropical Understory Bird Species Richness and
615 Abundance. *Conservation Biology*, 26(6), 1100–1111. doi:10.1111/j.1523-1739.2012.01940.x
- 616 McKenzie, D., & Kennedy, M. C. (2012). Power laws reveal phase transitions in landscape con-
617 trols of fire regimes. *Nat Commun*, 3, 726. Retrieved from <http://dx.doi.org/10.1038/ncomms1731>
618 http://www.nature.com/ncomms/journal/v3/n3/suppinfo/ncomms1731{__}S1.html
- 619 Mitchell, M. G. E., Suarez-Castro, A. F., Martinez-Harms, M., Maron, M., McAlpine, C., Gaston, K. J., ...
620 Rhodes, J. R. (2015). Reframing landscape fragmentation's effects on ecosystem services. *Trends in Ecology*
621 & Evolution, 30(4), 190–198. doi:10.1016/j.tree.2015.01.011
- 622 Naito, A. T., & Cairns, D. M. (2015). Patterns of shrub expansion in Alaskan arctic river corridors suggest
623 phase transition. *Ecology and Evolution*, 5(1), 87–101. doi:10.1002/ece3.1341
- 624 Newman, M. E. J. (2005). Power laws, Pareto distributions and Zipf's law. *Contemporary Physics*, 46(5),
625 323–351. doi:10.1080/00107510500052444
- 626 Oborny, B., Meszéna, G., & Szabó, G. (2005). Dynamics of Populations on the Verge of Extinction. *Oikos*,
627 109(2), 291–296. Retrieved from <http://www.jstor.org/stable/3548746>
- 628 Oborny, B., Szabó, G., & Meszéna, G. (2007). Survival of species in patchy landscapes: percolation in
629 space and time. In *Scaling biodiversity* (pp. 409–440). Cambridge University Press. Retrieved from <http://dx.doi.org/10.1017/CBO9780511814938.022>
- 631 Ochoa-Quintero, J. M., Gardner, T. A., Rosa, I., de Barros Ferraz, S. F., & Sutherland, W. J. (2015).
632 Thresholds of species loss in Amazonian deforestation frontier landscapes. *Conservation Biology*, 29(2),
633 440–451. doi:10.1111/cobi.12446
- 634 Ódor, G. (2004). Universality classes in nonequilibrium lattice systems. *Reviews of Modern Physics*, 76(3)

- 635 I), 663–724. doi:10.1103/RevModPhys.76.663
- 636 Pardini, R., Bueno, A. de A., Gardner, T. A., Prado, P. I., & Metzger, J. P. (2010). Beyond the Fragmen-
637 tation Threshold Hypothesis: Regime Shifts in Biodiversity Across Fragmented Landscapes. *PLoS ONE*,
638 5(10), e13666. doi:10.1371/journal.pone.0013666
- 639 Potapov, P., Yaroshenko, A., Turubanova, S., Dubinin, M., Laestadius, L., Thies, C., ... Zhuravleva, I. (2008).
640 Mapping the world's intact forest landscapes by remote sensing. *Ecology and Society*, 13(2).
- 641 Pueyo, S., de Alencastro Graça, P. M. L., Barbosa, R. I., Cots, R., Cardona, E., & Fearnside, P. M. (2010).
642 Testing for criticality in ecosystem dynamics: the case of Amazonian rainforest and savanna fire. *Ecology
Letters*, 13(7), 793–802. doi:10.1111/j.1461-0248.2010.01497.x
- 643 R Core Team. (2015). R: A Language and Environment for Statistical Computing. Vienna, Austria: R
644 Foundation for Statistical Computing. Retrieved from <http://www.r-project.org/>
- 645 Reyer, C. P. O., Rammig, A., Brouwers, N., & Langerwisch, F. (2015). Forest resilience, tipping points and
646 global change processes. *Journal of Ecology*, 103(1), 1–4. doi:10.1111/1365-2745.12342
- 647 Rockstrom, J., Steffen, W., Noone, K., Persson, A., Chapin, F. S., Lambin, E. F., ... Foley, J. A. (2009). A
648 safe operating space for humanity. *Nature*, 461(7263), 472–475. Retrieved from [http://dx.doi.org/10.1038/461472a](http://dx.doi.org/10.1038/
649 461472a)
- 650 Rooij, M. M. J. W. van, Nash, B., Rajaraman, S., & Holden, J. G. (2013). A Fractal Approach to Dynamic
651 Inference and Distribution Analysis. *Frontiers in Physiology*, 4(1). doi:10.3389/fphys.2013.00001
- 652 Saravia, L. A., & Momo, F. R. (2017). Biodiversity collapse and early warning indicators in
653 a spatial phase transition between neutral and niche communities. *PeerJ PrePrints*, 5, e1589v4.
654 doi:10.7287/peerj.preprints.1589v3
- 655 Scanlon, T. M., Caylor, K. K., Levin, S. A., & Rodriguez-iturbe, I. (2007). Positive feedbacks promote
656 power-law clustering of Kalahari vegetation. *Nature*, 449(September), 209–212. doi:10.1038/nature06060
- 657 Scheffer, M., Bascompte, J., Brock, W. A., Brovkin, V., Carpenter, S. R., Dakos, V., ... Sugihara, G. (2009).
658 Early-warning signals for critical transitions. *Nature*, 461(7260), 53–59. doi:10.1038/nature08227
- 659 Scheffer, M., Walker, B., Carpenter, S., Foley, J. a, Folke, C., & Walker, B. (2001). Catastrophic shifts in
660 ecosystems. *Nature*, 413(6856), 591–596. doi:10.1038/35098000
- 661 Seidler, T. G., & Plotkin, J. B. (2006). Seed Dispersal and Spatial Pattern in Tropical Trees. *PLoS Biology*,
- 662

- 663 4(11), e344. doi:10.1371/journal.pbio.0040344
- 664 Sexton, J. O., Noojipady, P., Song, X.-P., Feng, M., Song, D.-X., Kim, D.-H., ... Townshend, J. R.
665 (2015). Conservation policy and the measurement of forests. *Nature Climate Change*, 6(2), 192–196.
666 doi:10.1038/nclimate2816
- 667 Sexton, J. O., Song, X.-P., Feng, M., Noojipady, P., Anand, A., Huang, C., ... Townshend, J. R. (2013).
668 Global, 30-m resolution continuous fields of tree cover: Landsat-based rescaling of MODIS vegetation con-
669 tinuous fields with lidar-based estimates of error. *International Journal of Digital Earth*, 6(5), 427–448.
670 doi:10.1080/17538947.2013.786146
- 671 Sole, R. V., Alonso, D., & Mckane, A. (2002). Self-organized instability in complex ecosystems. *Philoso-
672 sophical Transactions of the Royal Society of London. Series B, Biological Sciences*, 357(May), 667–681.
673 doi:10.1098/rstb.2001.0992
- 674 Solé, R. V. (2011). *Phase Transitions* (p. 223). Princeton University Press. Retrieved from <https://books.google.com.ar/books?id=8RcLuv-Ll2kC>
- 676 Solé, R. V., & Bascompte, J. (2006). *Self-organization in complex ecosystems* (p. 373). New Jersey, USA.:
677 Princeton University Press. Retrieved from <http://books.google.com.ar/books?id=v4gpGH6Gv68C>
- 678 Solé, R. V., Alonso, D., & Saldaña, J. (2004). Habitat fragmentation and biodiversity collapse in neutral
679 communities. *Ecological Complexity*, 1(1), 65–75. doi:10.1016/j.ecocom.2003.12.003
- 680 Solé, R. V., Bartumeus, F., & Gamarra, J. G. P. (2005). Gap percolation in rainforests. *Oikos*, 110(1),
681 177–185. doi:10.1111/j.0030-1299.2005.13843.x
- 682 Stauffer, D., & Aharony, A. (1994). *Introduction To Percolation Theory* (p. 179). London: Taylor & Francis.
- 683 Staver, A. C., Archibald, S., & Levin, S. A. (2011). The Global Extent and Determinants of Savanna and
684 Forest as Alternative Biome States. *Science*, 334(6053), 230–232. doi:10.1126/science.1210465
- 685 Vasilakopoulos, P., & Marshall, C. T. (2015). Resilience and tipping points of an exploited fish population
686 over six decades. *Global Change Biology*, 21(5), 1834–1847. doi:10.1111/gcb.12845
- 687 Verbesselt, J., Umlauf, N., Hirota, M., Holmgren, M., Van Nes, E. H., Herold, M., ... Scheffer, M. (2016). Re-
688 motely sensed resilience of tropical forests. *Nature Climate Change*, 1(September). doi:10.1038/nclimate3108
- 689 Villa Martín, P., Bonachela, J. A., & Muñoz, M. A. (2014). Quenched disorder forbids discontinuous
690 transitions in nonequilibrium low-dimensional systems. *Physical Review E*, 89(1), 12145. Retrieved from

- 691 <https://link.aps.org/doi/10.1103/PhysRevE.89.012145>
- 692 Villa Martín, P., Bonachela, J. A., Levin, S. A., & Muñoz, M. A. (2015). Eluding catastrophic shifts.
- 693 *Proceedings of the National Academy of Sciences*, 112(15), E1828–E1836. doi:10.1073/pnas.1414708112
- 694 Viña, A., McConnell, W. J., Yang, H., Xu, Z., & Liu, J. (2016). Effects of conservation policy on China's
695 forest recovery. *Science Advances*, 2(3), e1500965. Retrieved from <http://advances.sciencemag.org/content/2/3/e1500965.abstract>
- 696
- 697 Vuong, Q. H. (1989). Likelihood Ratio Tests for Model Selection and Non-Nested Hypotheses. *Econometrica*,
698 57(2), 307–333. doi:10.2307/1912557
- 699 Weerman, E. J., Van Belzen, J., Rietkerk, M., Temmerman, S., Kéfi, S., Herman, P. M. J., & Koppell, J. V.
700 de. (2012). Changes in diatom patch-size distribution and degradation in a spatially self-organized intertidal
701 mudflat ecosystem. *Ecology*, 93(3), 608–618. doi:10.1890/11-0625.1
- 702 Weissmann, H., & Shnerb, N. M. (2016). Predicting catastrophic shifts. *Journal of Theoretical Biology*, 397,
703 128–134. doi:10.1016/j.jtbi.2016.02.033
- 704 Wuyts, B., Champneys, A. R., & House, J. I. (2017). Amazonian forest-savanna bistability and human
705 impact. *Nature Communications*, 8(May), 15519. doi:10.1038/ncomms15519
- 706 Xu, C., Hantson, S., Holmgren, M., Nes, E. H. van, Staal, A., & Scheffer, M. (2016). Remotely sensed
707 canopy height reveals three pantropical ecosystem states. *Ecology*, 97(9), 2518–2521. doi:10.1002/ecy.1470
- 708 Zhang, J. Y., Wang, Y., Zhao, X., Xie, G., & Zhang, T. (2005). Grassland recovery by protection from
709 grazing in a semi-arid sandy region of northern China. *New Zealand Journal of Agricultural Research*, 48(2),
710 277–284. doi:10.1080/00288233.2005.9513657
- 711 Zinck, R. D., & Grimm, V. (2009). Unifying wildfire models from ecology and statistical physics. *The
712 American Naturalist*, 174(5), E170–85. doi:10.1086/605959